Selfassembly of metallic nanoparticle arrays by DNA scaffolding

Shoujun Xiao[1,2], Furong Liu[3], Abbey E. Rosen[2], James F. Hainfeld[4], Nadrian C. Seeman[3],
Karin Musier-Forsyth[2] and Richard A. Kiehl[1,*]
[1]*Electrical and Computer Engineering Department,* [2]*Chemistry Department, University of Minnesota,
Minneapolis, MN 55455, USA;* [3]*Chemistry Department, New York University, New York,
NY 10003, USA;* [4]*Biology Department, Brookhaven National Laboratory, Upton, NY 11973, USA;*
*Author for correspondence (E-mail: kiehl@ece.umn.edu)

Abstract

We report the self-assembly of metallic nanoparticle arrays using DNA crystals as a programmable molecular scaffolding. Gold nanoparticles, 1.4 nm in diameter, are assembled in two-dimensional arrays with interparticle spacings of 4 and 64 nm. The nanoparticles form precisely integrated components, which are covalently bonded to the DNA scaffolding. These results show that heterologous chemical systems can be assembled into precise, programmable geometrical arrangements by DNA scaffolding, thereby representing a critical step toward the realization of DNA nanotechnology.

Several schemes in which DNA is used to assemble nanoparticles in specific geometrical arrangements have been reported, including (1) the formation of nanoparticle dimers and trimers by the attachment of nanoparticles to a single strand of DNA and subsequent hybridization to a target (Alivisatos et al., 1996), (2) the assembly of nanoparticles by using DNA as a selective adhesion material for 'gluing' objects together (Mirkin, 1996), and (3) the formation of supramolecular aggregates by self-assembly of DNA-streptavidin adducts (Niemeyer, 1998). The real potential of DNA nanotechnology will be realized, however, only when heterologous chemical systems have been scaffolded into precise, programmable geometrical arrangements. In this paper, we exploit the predictability of the local product structure in sticky-ended cohesion (Qiu et al., 1997) to construct two-dimensional (2D) structures comprising DNA crystals with covalently bonded metallic nanoparticles, which represent integrated nanocomponents.

Our approach exploits the work of Liu et al. (1999) in which 2D DNA crystals with modified surface features were constructed by tiling together rigid DNA motifs composed of double-crossover (DX) molecules containing DNA hairpins (Liu et al., 1999; Winfree et al., 1998). The use of 2D DNA crystals as a scaffolding potentially offers fundamental advantages over other self-assembly approaches with regard to the precision, rigidity, and programmabilty of the assembled nanostructures. On the other hand, this approach presents significant challenges because the unusual DNA motifs employed for DNA tiling appear to require aqueous environments containing significant concentrations of multivalent cations. These conditions are far from those commonly used when dealing with the components of potential interest for nanoelectronic applications, such as metallic nanoparticles and carbon nanotubes.

2D DNA crystals were formed by the assembly of a set of 22 specifically designed synthetic oligonucleotides in solution. The strands form four types of DX molecules, referred to as A, B, C, D in Figure 1. Molecules B and D are designed to have structural features protruding perpendicular to the crystal plane. In our approach, one of the protruding structures in the
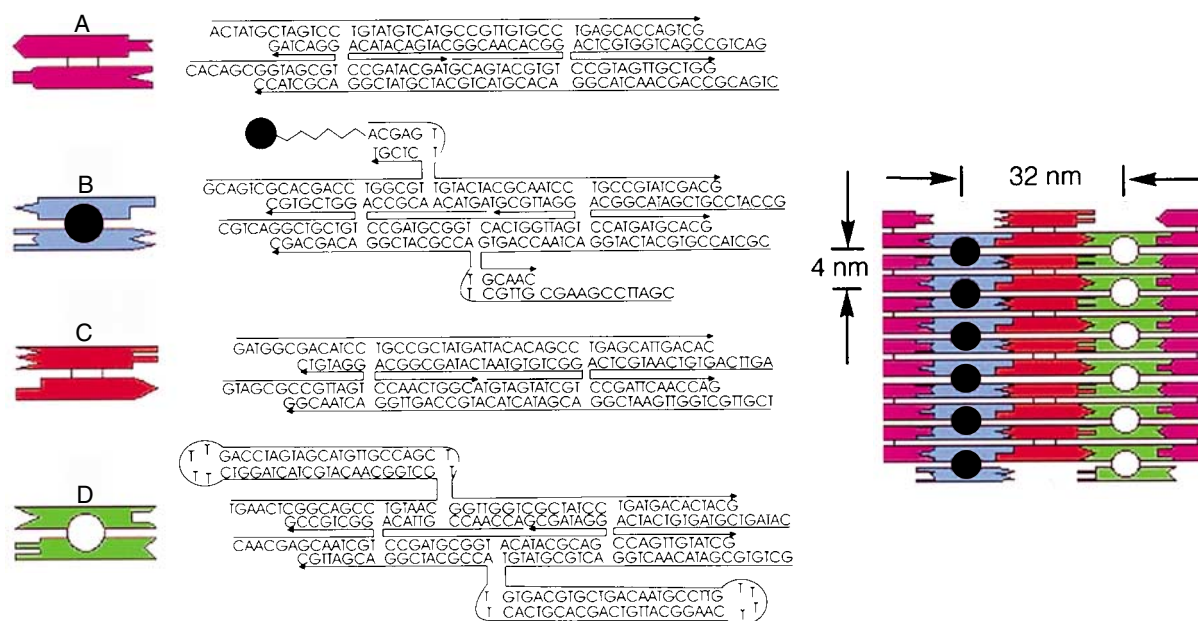
Figure 1. Sequences of the four DX molecules (A–D) and the tiling pattern used to assemble the 2D DNA crystals used in this work. The sequences of the 22 DNA strands including the DNA–Au conjugate (35-mer present in tile B; covalently attached gold nanoparticle indicated by a filled circle) are shown along with symbolic representations to the left. The 3′ end of each strand is indicated by an arrowhead. Molecules B and D each contain two protruding structures that extend out of the crystal plane, one above and one below the plane. The open and filled circles in the figure represent the protruding structures on one side (e.g. above) the plane. In the final DNA assembly shown at the far right, the spacing between these features is 32 nm in the horizontal direction and 4 nm in the vertical direction.

B molecule is exploited to incorporate nanoparticles into the crystal. The four types of DX molecules are designed to self-assemble by sticky-ended cohesion so as to tile the plane, thereby forming the 2D crystal shown schematically in Figure 1. The spacing between the B and D molecules in the crystal is 32 nm, while the spacing between identical molecules (A–A, B–B, etc.) in the perpendicular direction is 4 nm.

The Au nanoparticle used in this study is comprised of a Au_{55} cluster passivated with a phosphine ligand shell that is functionalized with a single reactive maleimide group (Monomaleimido Nanogold®, Nanoprobes, Stony Brook, NY). The diameter of the cluster and the thickness of the ligand shell are approximately 1.4 and 0.6 nm, respectively. DNA–Au conjugates were formed by covalently attaching a Au nanoparticle to the 5′ end of a thiol-containing DNA oligonucleotide that is part of one of the protruding structures of tile B, as illustrated in Figure 1. Our design includes a six-carbon linker to provide a separation between the nanoparticle (shown as a filled circle in Figure 1, tile B) and the oligonucleotide.

The DNA–Au conjugates were prepared from trityl-protected 5′-thiol-modified C6 oligonucleotides which were deprotected and reacted with monomaleimido-gold nanoparticles. A trityl-protected 5′-thiol-modified C6 oligonucleotide (TrS-$(CH_2)_6$-5′-ACGAGTTTG-TACTACGCAATCCTGCCGTATCGACG-3′, where Tr = trityl) was obtained from the University of Wisconsin Biotechnology Center and deprotected according to standard protocols (Glen Research, Sterling, VA). The conjugate was prepared by combining 6 nmol of deprotected DNA oligonucleotide and 6–12 nmol monomaleimido-gold nanoparticles (Nanoprobes, Inc) in 200 μl reaction buffer (20 mM NaH_2PO_4, 150 mM NaCl, 1 mM EDTA, pH 6.8). After incubation at room temperature for 1 h, the unreacted Au nanoparticles were separated from the unreacted DNA and DNA–Au conjugate by addition of 3 M sodium acetate (20 μl) and ice cold absolute ethanol (500 μl). This mixture was incubated at −20°C for 1–2 h, and then centrifuged at 4°C in a microcentrifuge set at 13 000 rpm for 15 min. The yellow supernatant containing the free Au nanoparticles was removed, and

the dark precipitate was dissolved in 90 µl of water and injected into a C4 reversed-phase HPLC column (Vydac, 5 µm, 30 nm; 0.46 × 25 cm^2). Chromatograms were developed at 0.8 ml/min with a CH$_3$CN gradient in 0.1 M aqueous triethylammonium acetate (TEAA) pH 6.5. From analysis of the HPLC chromatograms in Figure 2, the DNA : Au labeling stoichiometry of the purified conjugate was estimated to be 1 : 2, which is very close to the desired 1:1 product.

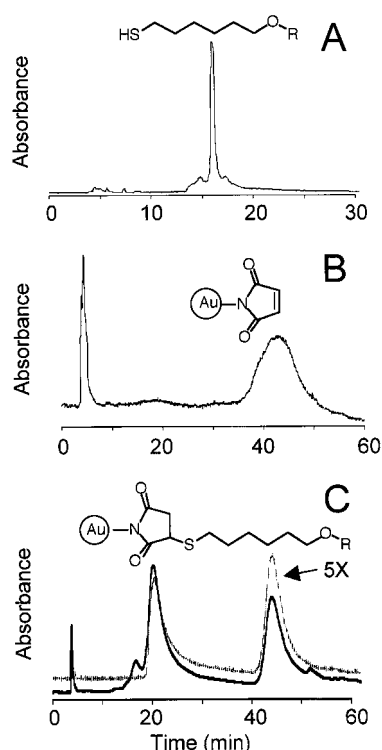2D DNA crystals containing Au nanoparticles were formed by slowly cooling a solution containing the

Figure 2. HPLC chromatograms of DNA–Au conjugate. The unreacted free sulfhydryl-containing oligonucleotide eluted as a sharp peak at 16 min (A), whereas the free monomaleimido-gold nanoparticles eluted as a broad peak centered at 43 min (B). The profile of the crude reaction mixture following the ethanol precipitation step described above was monitored at 260 nm ((C), thick line) and 350 nm ((C), thin line). The two major products, which eluted as broad peaks centered at 21 and 45 min, were collected, concentrated by lyophilization, desalted using Nap-5 columns (Pharmacia), and characterized by UV-visible spectrometry. This analysis suggested that conjugated DNA–Au at an approximately 1 : 1 stoichiometry was present in the 21 min fraction, which was subsequently used for the Au–DNA-containing crystal assemblies reported here.

entire set of 22 strands shown in Figure 1 from a temperature of 45°C to room temperature. Details of the growth process are similar to those described elsewhere (Liu et al., 1999), except for a lower initial temperature, which was chosen to ensure the stability of the DNA–Au conjugate. The Au–DNA-containing crystals were assembled by combining the 22 oligonucleotides in assembly buffer (40 mM sodium cacodylate, 11 mM MgCl$_2$, and 1 mM EDTA, pH 7.4). The final reaction volume was 50 µl and the concentration of each oligonucleotide was 0.4 µM, with the exception of the Au–DNA strand, which was present at 0.8 µM. The reaction mixture was placed in a 2 liter water bath initially set at 45°C and then slowly cooled to room temperature by placing the beaker in an insulated styrofoam box for at least 24 h. Following this incubation, the mixture was transferred to a 50 µl AmiKa Biodialyzer and dialyzed overnight (12–15 h) against 500 ml of assembly buffer at 4°C using a 0.01 µm pore polycarbonate membrane (AmiKa). Crystals containing the same 22 strands but without the Au nanoparticle were also grown and were examined to confirm that the intended crystal structure was obtained. For this purpose, a higher initial growth temperature of 95°C was used to produce larger crystals, which was beneficial for visualization. Visualization of the 2D DNA crystals was carried out by atomic force microscopy (AFM), transmission electron microscopy (TEM), and scanning transmission electron microscopy (STEM).

TEM images were obtained using a JEOL 1210 instrument operated at 120 kV. The samples were prepared on 400 mesh copper grids with an ultra thin carbon film. The carbon grid was dried overnight and floated on a 2 µl drop of the DNA crystal solution. Staining was accomplished by sequentially floating the grid on four 50 µl drops of 0.1% uranyl acetate for 30 s each, and then wicking off the solution.

Figure 3A shows a TEM image of a large DNA crystal assembled without Au nanoparticles. The alternate dark-gray and light-gray bands in the image are the result of uranyl acetate staining. The major spacings (dark-to-dark and light-to-light) between gray bands in Figure 3A are in good agreement with the 64 nm design value for the B–B and D–D molecule spacings, while the minor spacings (dark-to-light) are in good agreement with the 32 nm design value of the B–D spacing.

AFM samples were prepared by spotting 3–5 µl of solution on freshly cleaved mica (Ted Pella) and waiting 2 min for adsorption to the surface. To remove buffer salts, 5–10 drops of distilled H$_2$O were placed

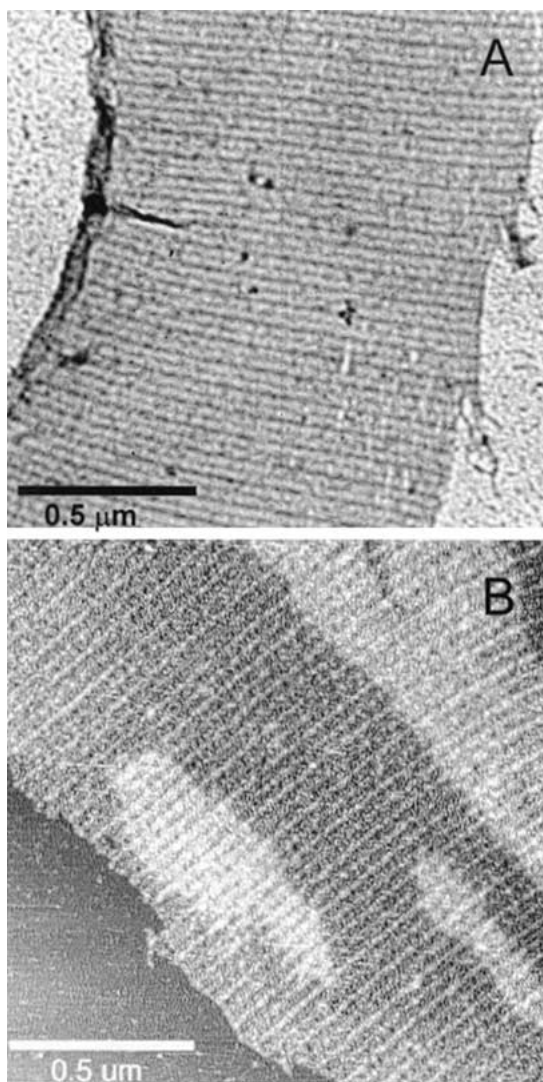*Figure 4*. Scanning TEM image of a DNA crystal incorporating the DNA–Au conjugate.

Figure 3. (A) TEM image and (B) AFM contact-mode image of 2D DNA crystals formed from the 22 strands of Figure 1 but without Au nanoparticles.

on the mica, the drop was shaken off and the sample was dried with compressed air. A Digital Instruments NanoScope® III with a JV-4042 scanning head was used for the AFM measurements. The sample was imaged in contact mode in an isopropanol fluid cell at a scanning frequency of 6.1 Hz using commercial Model NPS (Digital Instruments) Si_3N_4 cantilevers.

The AFM image in Figure 3B shows a similar banded pattern with alternation in lightness and spacings similar to those in the TEM image. The lighter regions in this contact mode AFM image correspond to higher
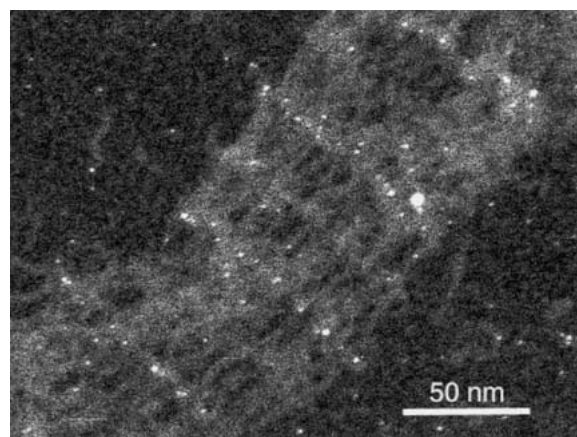
regions on the surface. Hence, the alternation in the lightness of the bands observed in both the TEM and AFM images can be attributed to the slight differences in the physical makeup of the protruding structures in molecules B and D.

To prepare STEM samples, a drop of the sample solution was applied to a thin 0.2 nm carbon film over a holey substrate on an EM grid. After 1 min of adsorption, the sample was rinsed several times with 20 mM ammonium acetate, then rapidly frozen in liquid nitrogen slush and freeze dried overnight. Grids were viewed in dark field with the high-performance field-emission Brookhaven STEM operating a 40 keV.

A darkfield STEM image of an unstained DNA crystal in which the DNA–Au conjugate was incorporated is shown in Figure 4. Both the DNA crystal and the Au nanoparticles are clearly visible in the STEM image. The figure shows that closely spaced Au nanoparticles are assembled into the DNA crystal along lines that are approximately 64 nm apart, consistent with the B–B spacing of our design. While distinct features are discernible in the structure of the DNA crystal midway between the lines of Au nanoparticles, no significant attachment of Au is observed at the midway points. This is consistent with the alternation of Au-decorated (B) molecules and undecorated (D) molecules in the crystal design. Based on the designed spacing between particles along the lines (4 nm), we estimate an attachment yield for the nanoparticles of about 70% for this image. Examination of the nanoparticle spacing in the regions of highest yield gives a value close to 4 nm, as expected. It may also be noted that the small deviation

in the position of the Au nanoparticles from their centerlines in Figure 4 is consistent with the small separation between the nanoparticle and its anchor position on the crystal associated with the 7-nucleotide, 6-carbon tether, which is slightly less than 4 nm. It is important to emphasize that the sample in Figure 4 was not stained or enhanced in any way, thereby eliminating the possibility of artifacts that might arise due to staining or other contrast enhancement techniques. Thus, this image provides an unambiguous confirmation that Au nanoparticles have been assembled into arrays by the DNA scaffolding.

We have demonstrated a capability for the assembly of periodic arrays of nanoparticles with nanometer-scale precision. The design flexibility offered by the programmability of the base sequence in synthetic DNA, together with the ultra-small scale associated with the 0.34 nm base-pair separation in the DNA helix, could lead to a technology for the 'bottom-up' assembly of components at dimensions far below the limits of conventional 'top-down' lithographic manufacturing techniques. The use of DNA crystals as a scaffolding within which nanoparticles (clusters, tubes, molecules) can precisely assemble provides a new basis for nanoscale manufacturing with applications in many fields, including nanoelectronics (Robinson & Seeman, 1987; Kiehl, 2000), nanorobotics, nanomaterials, and structural analysis (Seeman, 1982).

Acknowledgements

References

Alivisatos A.P. et al., 1996. Organization of nanocrystal molecules using DNA. Nature, 382, 609.

Kiehl R.A., 2000. Nanoparticle electronic architectures assembled by DNA. J. Nanoparticle Res. 2, 331.

Liu F., R. Sha & N.C. Seeman, 1999. Modifying the surface features of two-dimensional DNA crystals. J. Am. Chem. Soc. 121, 917.

Niemeyer C.M., W. Burger & J. Peplies, 1998. Streptavidin conjugates as building blocks for novel biometallic nanostructures. Angew. Chem., Int. Ed. Engl. 37, 2265.

Qiu H., J.C. Dewan & N.C. Seeman, 1997. A DNA decamer with a sticky end: The crystal structure of d-CGACGATCGT. J. Mol. Biol. 267, 881.

Robinson B.H. & N.C. Seeman, 1987. The design of a biochip: A self-assembling molecular-scale memory device. Prot. Eng. 1, 295.

Seeman N.C., 1982. Nucleic acid junctions and lattices. J. Theor. Biol. 99, 237.

Winfree E., F. Liu, L.A. Wenzler & N.C. Seeman, 1998. Design and self-assembly of two-dimensional DNA crystals. Nature 394, 539.